Effective longitudinal shear moduli of random composites comprising radially-graded fibres

Edoardo Artioli, Paolo Bisegna, Federica Caselli, Franco Maceri
Department of Civil Engineering, University of Rome "Tor Vergata", Italy
E-mail: {artioli, bisegna, caselli, maceri}@ing.uniroma2.it

Keywords: Functionally graded materials, fibre-reinforced composite materials, homogenization.

SUMMARY. The homogenization problem for random composites comprising radially-graded fibres is dealt with, in the framework of antiplane shear deformations, by generalizing the Rayleigh multipole expansion method. The statistics of the effective moduli are obtained in simulation. The feasibility of reducing the shear stress at the fibre/matrix interface by properly grading the fibre stiffness along the radius is proved.

1 INTRODUCTION

The homogenization problem for composites with long, parallel, randomly arranged fibres is dealt with here, in the framework of antiplane shear deformations. A peculiar feature of this study is that fibres are made of functionally graded material [1], i.e., they have composition which vary continuously along the radius, resulting in a corresponding variation of their stiffness, which can thus be tailored for reducing the stress level at the fibre/matrix interface.

A repeating unit cell (RUC) of the material is considered (Figure 1), and periodic boundary conditions are enforced [2], by generalizing an approach tracing back to the classical Rayleigh multipole expansion method [3, 4, 5], to the present multiple-inclusion situation. In particular, the solution over the matrix domain is represented by superimposing the multipole expansions relevant to each fibre of the RUC, given by series of doubly-periodic functions arising from the theory of Weierstrass elliptic functions. The actual solution is then obtained through the identification of the above representation with the Fourier-series representation around each fibre. After satisfying the field equilibrium equation in the fibre and matrix domains, and enforcing the equilibrium and compatibility condition at the fibre/matrix interface, an infinite system of linear algebraic equations is derived, which is truncated to a finite order and numerically solved. The numerical implementation exhibits exponential asymptotic convergence rate with respect to the truncation order of the involved series representations. The proposed method is especially useful for composites comprising nearly touching fibres (e.g., Figure 1), since in those cases FEM solutions require extremely fine meshes to properly resolve the relevant narrow regions.

Monte Carlo simulations are used to approximate the statistics of the effective moduli. It is shown that for sufficiently large RUCs, no bias is introduced in the estimation by edge effects generated by the periodic boundary conditions. Hence, sufficiently large RUCs can be used to obtain a fair estimate of the effective moduli. However, a stochastic dispersion is inherent to different RUC realizations. A fit of the relevant standard deviation versus the RUC size is obtained in simulation, and used to estimate the number of realizations that must be generated, solved and averaged, in order to reach a required accuracy of the effective moduli.

These results enable the analysis of random composites comprising radially-graded fibres. It is shown that suitably tuning the fibre grading profile is a feasible way to reduce the shear stress at the fibre/matrix interfaces, without reducing the overall stiffness of the material. This outcome raises attention on the possibility of devising innovative composite materials, specifically designed to have

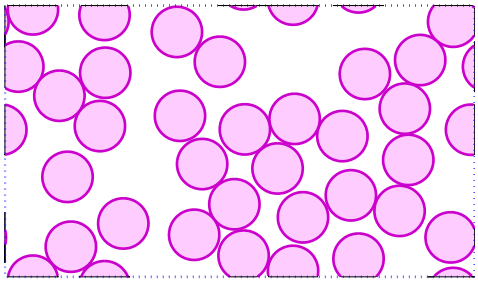

Figure 1: A stochastic realization of a repeating unit cell (RUC) of the composite.

better performance with respect to the risk of fibre/matrix debonding.

2 STATEMENT OF THE PROBLEM

Reference is made to a fibre-reinforced composite material, with long, parallel fibres, randomly distributed in the material with a statistically homogeneous microstructure. Fibres have a circular cross section and their radii may have a known random distribution.

A repeating unit cell (RUC) is considered, arranged in a periodic lattice. The RUC is assumed to be a parallelogram, with sides L_1 and L_2 forming an angle φ. It contains the centres of F fibres, denoted by C_j, with radii R_j, $j = 1 \dots F$.

The effective material shear moduli are obtained here by asymptotic homogenization: to this end, a family of problems is introduced, indexed by a parameter ε scaling the microstructure. The value $\varepsilon = 1$ refers to the real composite material under consideration, whereas the homogenization limit is obtained by letting the parameter ε go to zero.

In the framework of antiplane shear deformations, the problem of determining the longitudinal displacement field w_ε in the composite domain is stated as follows:

$$\operatorname{div}(\boldsymbol{G}\nabla w_\varepsilon) = 0\,, \qquad \text{in } \cup_j \Omega^{\mathrm{f}}_{j\varepsilon} \cup \Omega^{\mathrm{m}}_\varepsilon\,; \tag{1}$$

$$[\![\boldsymbol{G}\nabla w_\varepsilon \cdot \boldsymbol{\nu}]\!] = 0\,, \qquad \text{on } \cup_j \Gamma_{j\varepsilon}\,; \tag{2}$$

$$\boldsymbol{G}\nabla w_\varepsilon \cdot \boldsymbol{\nu} = \frac{1}{\varepsilon} D_j [\![w_\varepsilon]\!]\,, \qquad \text{on } \cup_j \Gamma_{j\varepsilon}\,. \tag{3}$$

Here $\cup_j \Omega^{\mathrm{f}}_{j\varepsilon}$ and $\Omega^{\mathrm{m}}_\varepsilon$ denote fibres and matrix domains respectively, $\cup_j \Gamma_{j\varepsilon}$ is the ensemble of fibre/matrix interfaces, $\boldsymbol{\nu}$ is the normal unit vector to $\cup_j \Gamma_{j\varepsilon}$ pointing into $\Omega^{\mathrm{m}}_\varepsilon$, and square brackets $[\![\,\cdot\,]\!]$ denote the jump of the enclosed quantity across the interface, defined as extra-fibre value minus intra-fibre value.

Equation (1) is the field equilibrium equation; (2) accounts for equilibrium at the fibre/matrix interface, stipulating the continuity of the normal-to-interface component of the shear stress; (3) describes the interface constitution law. These equations must be complemented by suitable boundary conditions on the boundary of the domain $\Omega = (\cup_j \Omega^{\mathrm{f}}_{j\varepsilon}) \cup (\cup_j \Gamma_{j\varepsilon}) \cup \Omega^{\mathrm{m}}_\varepsilon$, but their specification is immaterial for the present treatment.

Fibres and matrix are assumed to be linear elastic, and their shear moduli are collected in the constitutive tensor $\boldsymbol{G}$, which specializes in

$$\boldsymbol{G} = \boldsymbol{G}^{\mathrm{f}}_j \quad \text{in } \Omega^{\mathrm{f}}_{j\varepsilon}\,,\ j = 1 \dots F\,, \qquad \boldsymbol{G} = \boldsymbol{G}^{\mathrm{m}} \quad \text{in } \Omega^{\mathrm{m}}_\varepsilon\,. \tag{4}$$

The matrix material is homogeneous and isotropic, so that $\boldsymbol{G}^{\mathrm{m}} = G^{\mathrm{m}}\boldsymbol{I}$, with $\boldsymbol{I}$ the second order identity tensor and G^{m} the matrix shear modulus. Fibres are made of a linear elastic, cylindrically-orthotropic material whose moduli are functionally-graded along the radius. Introducing a polar coordinate system (C_j, r_j, θ_j), the fibre elasticity tensor is:

$$\boldsymbol{G}_j^{\mathrm{f}} = (G_j^{\mathrm{r}}\boldsymbol{e}_j^{\mathrm{r}} \otimes \boldsymbol{e}_j^{\mathrm{r}} + G_j^{\theta}\boldsymbol{e}_j^{\theta} \otimes \boldsymbol{e}_j^{\theta})g_j(\rho_j)\,, \tag{5}$$

where $\rho_j = r_j/R_j$ is the radial dimensionless coordinate, $\boldsymbol{e}_j^{\mathrm{r}}$ and $\boldsymbol{e}_j^{\theta}$ are the radial and tangential unit vectors, respectively, $\otimes$ denotes the tensor product, and the dimensionless functions $g_j(\rho_j)$ express the material grading law along the radial direction relevant to fibre j.

Fibre/matrix interfaces are assumed to have zero-thickness and to be imperfect. The linear spring-layer model, linearly relating the displacement discontinuity $[\![w_\varepsilon]\!]$ to the interface traction $\boldsymbol{G}\nabla w_\varepsilon \cdot \boldsymbol{\nu}$, in terms of the spring constant parameter D_j is adopted [6, 7, 8]. As a matter of fact, interfaces have a physical thickness t which, though much smaller than the microstructural length scale L_1 (or L_2) to justify the present zero-thickness model, rescales as the latter one during the homogenization process. Recalling that the corresponding interface parameter is inversely proportional to the interface thickness, the ε^{-1} scaling of the interface parameter in the homogenization limit follows [6, 9].

In order to guarantee the well posedness of the above problem, the following hypotheses are assumed:

$$G^{\mathrm{m}} > 0\,, \quad G_j^{\mathrm{r}} > 0\,, \quad G_j^{\theta} > 0\,, \quad D_j > 0\,, \quad g_j(\rho_j) > 0 \quad \text{in } (0,1]\,, \quad j = 1 \dots F. \tag{6}$$

2.1 *Homogenized equilibrium equation*

The asymptotic homogenization method is employed to derive the homogenized or effective constitutive tensor of the composite material. Two different length scales characterize the problem under consideration. Hence, two different space variables are introduced: the macroscopic one, x, and the microscopic one, $y = x/\varepsilon$, $y \in Q$, being Q the RUC (see Figure 1), whose extra-fibre space, intra-fibre space and fibre-matrix interface are denoted by Q^{m}, Q_j^{f} and Γ_j, for $j = 1 \dots F$, respectively. An asymptotic expansion of the unknown displacement field is considered in the form:

$$w_\varepsilon(x,y) = w_0(x,y) + \varepsilon w_1(x,y) + \varepsilon^2 w_2(x,y) + \dots\,, \tag{7}$$

where w_0, w_1, w_2 are Q-periodic functions in y, and w_1, w_2 have null integral average over Q. Substituting (7) into Problem (1)–(3) and equating the power-like terms of ε, three differential problems for w_0, w_1 and w_2 are obtained, respectively, which, following a standard argument [10, 11], yield the homogenized equation for the macroscopic displacement w_0:

$$\mathrm{div}_x(\boldsymbol{G}^{\#}\nabla_x w_0) = 0\,. \tag{8}$$

Here $\nabla_x w_0$ is the macroscopic shear strain, and

$$\boldsymbol{G}^{\#} = \frac{1}{|Q|}\int_Q \boldsymbol{G}(\boldsymbol{I} - \nabla_y^{\mathrm{t}}\boldsymbol{\chi})\,\mathrm{d}a \tag{9}$$

is the effective constitutive tensor, where the superscript $^{\mathrm{t}}$ denotes the transpose, $\mathrm{d}a$ is the area element of Q, $|\cdot|$ is the Lebesgue measure, and the cell function $\boldsymbol{\chi}(y)$ has been introduced. Its

components $\chi_h, h = 1, 2$, are the unique, null average, Q-periodic solutions of the cell problem:

$$\mathrm{div}_y[\boldsymbol{G}(\nabla_y \chi_h - \boldsymbol{e}_h)] = 0\,, \qquad \text{in } \cup_j Q_j^{\mathrm{f}} \cup Q^{\mathrm{m}}\,; \tag{10}$$

$$[\![\boldsymbol{G}(\nabla_y \chi_h - \boldsymbol{e}_h) \cdot \boldsymbol{\nu}]\!] = 0\,, \qquad \text{on } \cup_j \Gamma_j\,; \tag{11}$$

$$\boldsymbol{G}(\nabla_y \chi_h - \boldsymbol{e}_h) \cdot \boldsymbol{\nu} = D_j [\![\chi_h]\!]\,, \qquad \text{on } \cup_j \Gamma_j\,, \tag{12}$$

where $\boldsymbol{e}_h$ is the unit vector parallel to the y_h axis.

Using the Gauss-Green Lemma and introducing the auxiliary cell function:

$$\tilde{\boldsymbol{\chi}} = \boldsymbol{\chi} - (y_1 \boldsymbol{e}_1 + y_2 \boldsymbol{e}_2)\,, \tag{13}$$

(9) is transformed into:

$$\boldsymbol{G}^{\#} = \boldsymbol{G}^{\mathrm{m}} + \sum_{j=1}^{F} \frac{1}{|Q|} \int_{Q_j^{\mathrm{f}}} (\mathrm{div}_y \boldsymbol{G}^{\mathrm{f}}) \otimes \tilde{\boldsymbol{\chi}}\, \mathrm{d}a + \sum_{j=1}^{F} \frac{1}{|Q|} \int_{\Gamma_j} [\![\boldsymbol{G}\boldsymbol{\nu} \otimes \tilde{\boldsymbol{\chi}}]\!]\, \mathrm{d}l\,. \tag{14}$$

where $\mathrm{d}l$ is the line element of Γ_j. Equation (14) yields the effective shear moduli of the composite material in terms of the solution $\boldsymbol{\chi}$ of the cell problem.

In applications, a central role is played by the local shear stress $\boldsymbol{\tau}_\varepsilon = \boldsymbol{G}\nabla w_\varepsilon$ in the composite. The leading-order term of its asymptotic expansion turns out to be:

$$\boldsymbol{\tau}_0 = \boldsymbol{G}(\boldsymbol{I} - \nabla_y^{\mathrm{t}} \boldsymbol{\chi})[\nabla_x w_0]\,. \tag{15}$$

This expression will be used in Section 4.2, dealing with stress concentration issues.

3 CELL PROBLEM

3.1 *Fourier series representation*

The general solution of the field equation (10) is obtained via Fourier series representations. With reference to fibre j, $j = 1 \ldots F$, the cell function χ_h, $h = 1, 2$, is given by:

- in the isotropic, homogeneous matrix subdomain Q^{m}:

$$\chi_{jh}^{\mathrm{m}}(r_j, \theta_j) = y_h + \Re \left[\sum_{k=-\infty}^{+\infty} b_{kjh} \rho_j^k \mathrm{e}^{\mathrm{i}k\theta_j} \right]\,, \tag{16}$$

- in the cylindrically orthotropic, radially-graded fibre subdomain Q_j^{f}:

$$\chi_{jh}^{\mathrm{f}}(r_j, \theta_j) = y_h + \Re \left[\sum_{k=0}^{+\infty} a_{kjh}\, W_{kj}(\rho_j) \mathrm{e}^{\mathrm{i}k\theta_j} \right]\,. \tag{17}$$

Here $\mathrm{i} = \sqrt{-1}$ and the symbol $\Re$ denotes the real part; moreover, the sum in (17) is extended over nonnegative indices only, in order to enforce the regularity of χ_{jh}^{f} near $C_j \in Q_j^{\mathrm{f}}$. Finally, functions $W_{kj}(\rho_j)$ solve the problem:

$$W_{kj}'' + \left(\frac{g_j'}{g_j} + \frac{1}{\rho_j} \right) W_{kj}' - \frac{\sigma_j^2 k^2}{\rho_j^2} W_{kj} = 0\,, \quad \text{in } (0, 1)\,, \tag{18}$$

$$W_{kj}(0) = 0\,, \tag{19}$$

$$W_{kj}(1) = 1\,, \tag{20}$$

where (19) is a regularity requirement on W_{kj}, (20) is a normalization condition, $\sigma_j^2 = G_j^\theta / G_j^{\mathrm{r}}$ is the anisotropy ratio of fibre j, and an apex denotes differentiation with respect to ρ_j. Finally, the quantities a_{kjh}, b_{kjh}, $b_{(-k)jh}$, $k = 1, \ldots, +\infty$, are complex constants, whilst a_{0jh} and b_{0jh} are real constants. They are determined in Sections 3.2 and 3.3, by exploiting the interface boundary conditions (11)-(12) on Γ_j and the periodicity requirement on ∂Q.

3.2 *Interface boundary condition*

Substituting representations (16)–(17) into the interface boundary conditions (11)–(12), the following equations are obtained for $k = 1 \ldots + \infty$:

$$G^{\mathrm{m}} k R_j^{-1} (b_{kjh} - \overline{b}_{(-k)jh}) = G_j^{\mathrm{r}} g_j(1) W'_{kj}(1) R_j^{-1} a_{kjh} \,, \tag{21}$$

$$D_j (b_{kjh} + \overline{b}_{(-k)jh} - a_{kjh}) = G_j^{\mathrm{r}} g_j(1) W'_{kj}(1) R_j^{-1} a_{kjh} \,, \tag{22}$$

whereas $k = 0$ yields $b_{0jh} = a_{0jh}$. Here an overbar denotes the complex conjugate. Equations (21)–(22) allow to express the unknown coefficients a_{kjh} and b_{kjh} as functions of $b_{(-k)jh}$, as follows:

$$a_{kjh} = \lambda_{kj} \overline{b}_{(-k)jh} \,, \qquad b_{kjh} = \gamma_{kj} \overline{b}_{(-k)jh} \,, \tag{23}$$

where

$$\lambda_{kj} = \frac{2 R_j D_j [G_j^{\mathrm{r}} g_j(1)]^{-1}}{k + \psi_{kj}^-} \, \frac{k}{W'_{kj}(1)} \,, \qquad \gamma_{kj} = \frac{k + \psi_{kj}^+}{k + \psi_{kj}^-} \,, \tag{24}$$

being

$$\psi_{kj}^{\pm} = R_j D_j \left\{ \frac{k}{W'_{kj}(1)} [G_j^{\mathrm{r}} g_j(1)]^{-1} \pm (G^{\mathrm{m}})^{-1} \right\} . \tag{25}$$

3.3 *Periodicity condition*

The cell function $\boldsymbol{\chi}$ is Q-periodic, i.e., it satisfies:

$$\boldsymbol{\chi}(y_1 + L_1, y_2) = \boldsymbol{\chi}(y_1, y_2) = \boldsymbol{\chi}(y_1 + L_2 \cos\varphi, y_2 + L_2 \sin\varphi) \,. \tag{26}$$

It is sufficient to enforce this periodicity requirement with reference to the restriction of $\boldsymbol{\chi}$ to the matrix domain Q^{m}. This is obtained by identifying the representation (16) with a linear combination of doubly-periodic basis functions defined in terms of the complex variable $z = (y_1 + \mathrm{i} y_2)/L_1$. Accordingly, the relevant semi-periods are $\omega_1 = 1/2$, $\omega_2 = \kappa \mathrm{e}^{\mathrm{i}\varphi}/2$, where $\kappa = L_2/L_1$ is the side ratio of the RUC. More specifically, according to the classical Rayleigh multipole expansion method [3, 12], the following equation is implemented:

$$\chi_h^{\mathrm{m}}(z) = \sum_{n=1}^{F} \sum_{l=1}^{2} \sum_{s=1}^{+\infty} w_{slnh} \, \Re[B_{sl}(z - z_n)] \,. \tag{27}$$

Here z_n is the value of z corresponding to the centre C_n of fibre n, the coefficients w_{slnh} are real unknowns, and the functions $B_{sl}(z)$ are chosen as follows [13, 14, 5, 15]:

$$B_{sl}(z) = \begin{cases} -\eta_l z + \omega_l \zeta(z) \,, & \text{if } s = 1, \ l = 1, 2 \,; \\ \omega_l \frac{\zeta^{(s-1)}(z)}{(s-1)!} \,, & \text{for } s > 1, \ l = 1, 2 \,, \end{cases} \tag{28}$$

where $\zeta(z)$ denotes the Weierstrass Zeta function of semiperiods ω_1, ω_2 [16]. It is odd and quasi-periodic, i.e., $\zeta(z+2\omega_k) = \zeta(z) + 2\eta_k$, with $k = 1, 2$, and $\eta_k = \zeta(\omega_k)$. The latter quantities are linked to the semiperiods ω_1, ω_2 by Legendre's relationship $\eta_1\omega_2 - \eta_2\omega_1 = \pi\mathrm{i}/2$. Using these equations, and recalling that the derivatives of $\zeta(z)$ are elliptic functions, it is easy to verify that the basis functions $\Re[B_{sl}(z - z_n)]$ are indeed doubly periodic, with semiperiods ω_1, ω_2.

In the cited literature, the RUC is symmetric with respect to the y_1 and y_2 axes. This implies evenness or oddness properties for the cell function χ_h^{m}, which is consequently represented by the subset of the functions (28) corresponding to $l = 1$ or $l = 2$ only. In this work no such symmetry is assumed, and hence the whole set (28) is considered. Moreover, a superposition of multipoles around each fibre is taken into account.

The identification of (16) and (27) is easily obtained by introducing power-series expansions around $z = z_j$ of the functions $B_{sl}(z - z_n)$ and remembering that

$$z - z_j = \frac{r_j \mathrm{e}^{\mathrm{i}\theta_j}}{L_1} = \hat{R}_j \rho_j \mathrm{e}^{\mathrm{i}\theta_j}\,, \tag{29}$$

where $\hat{R}_j = R_j/L_1$ is the dimensionless fibre radius. In particular, $\zeta(z)$ has a pole of order 1 at $z = 0$, and its Laurent series expansion is:

$$\zeta(z) = \frac{1}{z} - \sum_{k=2}^{+\infty} c_k \frac{z^{2k-1}}{2k-1}\,, \tag{30}$$

where c_k, $k \geq 2$ can be easily computed using a rapidly convergent Fourier series [17]. Accordingly, the power-series expansion of $\zeta^{s-1}(z - z_j)$, $s \geq 1$, around $z = z_j$ is given by:

$$\frac{\zeta^{s-1}(z - z_j)}{(s-1)!} = (-1)^{s-1}(z - z_j)^{-s} - \sum_{k=0}^{+\infty} \mu_{ks}(z - z_j)^k\,, \tag{31}$$

where

$$\mu_{ks} = \begin{cases} \frac{1}{k+s-1}\binom{k+s-1}{s-1}\, c_{\frac{k+s}{2}}\,, & \text{for even } k+s\,; \\ 0\,, & \text{for odd } k+s\,. \end{cases} \tag{32}$$

Here round brackets denote the binomial coefficient, and it has been stipulated that $c_1 = 0$ for ease of notation. On the other hand, $\zeta(z - z_n)$, for $n \neq j$, is analytic around $z = z_j$, and its Taylor expansion is:

$$\zeta^{s-1}(z - z_n) = \sum_{k=0}^{+\infty} \frac{\zeta^{k+s-1}(z_j - z_n)}{k!}(z - z_j)^k\,. \tag{33}$$

Hence, (27) is transformed into:

$$\chi_h^{\mathrm{m}}(z) = \Re\left[C_{0jh} + \sum_{k=1}^{+\infty} C_{(-k)jh}(z - z_j)^{-k} + \sum_{k=1}^{+\infty} C_{kjh}(z - z_j)^k\right]\,, \tag{34}$$

where, for $k = 1, \ldots, +\infty$,

$$C_{(-k)jh} = (-1)^{k-1} \sum_{l=1}^{2} w_{kljh}\, \omega_l \,, \tag{35}$$

$$C_{kjh} = \sum_{\substack{n=1 \\ n\neq j}}^{F} \sum_{l=1}^{2} \sum_{s=1}^{+\infty} w_{slnh}\, \omega_l \frac{\zeta^{k+s-1}(z_j - z_n)}{(s-1)!k!} - \sum_{l=1}^{2} \sum_{s=1}^{+\infty} w_{sljh}\, \omega_l\, \mu_{ks}$$
$$- \delta_{k1} \sum_{n=1}^{F} \sum_{l=1}^{2} w_{1lnh}\, \eta_l \,, \tag{36}$$

where δ is the Krönecker symbol. The expression of C_{0jh} is obtained by setting $k = 0$ in the expression of C_{kjh}, and adding the constant term $\sum_{n=1}^{F} \sum_{l=1}^{2} -w_{1lnh}\, \eta_l (z_j - z_n)$.

Equation (34), recalling (29), is compared term-by-term to (16) and yields, for $k = 1 \ldots + \infty$:

$$b_{(-k)jh} = \hat{R}_j^{-k} C_{(-k)jh} \,, \tag{37}$$

$$b_{kjh} + R_j c_h \delta_{k1} = \hat{R}_j^{k} C_{kjh} \,, \tag{38}$$

$$b_{0jh} + y_h^{C_j} = C_{0jh} \,, \tag{39}$$

where $y_h^{C_j}$ is the y_h coordinate at the centre C_j of fibre j, and $c_h = 1$ if $h = 1$, $c_h = -\mathrm{i}$ if $h = 2$, so that $y_h = y_h^{C_j} + \Re(c_h r_j \mathrm{e}^{\mathrm{i}\theta_j})$.

3.4 *Solution of the cell problem and effective constitutive tensor*

The solution of the cell problem is achieved by substituting (37)–(38) into the interface boundary condition $(23)_2$, leading to:

$$\hat{R}_j^{k} C_{kjh} - R_j c_h \delta_{k1} = \gamma_{kj} \hat{R}_j^{-k} \overline{C}_{(-k)jh} \,. \tag{40}$$

This is a system of infinite linear algebraic equations in the unknowns w_{kljh}, involved into C_{kjh} and $C_{(-k)jh}$. Making the position [18]

$$q_{kljh} = \frac{\sqrt{k}}{\hat{R}_j^{k}} w_{kljh} \,, \tag{41}$$

and recalling (35) and (36), (40) yields, after multiplying by $-\sqrt{k}$:

$$(-1)^{k-1} \gamma_{kj} \sum_{l=1}^{2} \overline{\omega}_l\, q_{kljh} - \sum_{\substack{n=1 \\ n\neq j}}^{F} \sum_{l=1}^{2} \sum_{s=1}^{+\infty} \sqrt{\frac{k}{s}} \omega_l \hat{R}_j^{k} \hat{R}_n^{s} \frac{\zeta^{k+s-1}(z_j - z_n)}{(s-1)!k!}\, q_{slnh}$$
$$+ \sum_{l=1}^{2} \sum_{s=1}^{+\infty} \sqrt{\frac{k}{s}} \omega_l \mu_{ks} \hat{R}_j^{k+s}\, q_{sljh} + \delta_{k1} \sum_{n=1}^{F} \sum_{l=1}^{2} \hat{R}_j \hat{R}_n \eta_l\, q_{1lnh} = -R_j c_h \delta_{k1} \,. \tag{42}$$

To obtain a numerical solution, it is necessary to truncate this system to a finite order N, amounting to extending the sums in the representations (16)–(17) to $|k| \leq N$ only.

Recalling that (42) hold for $j = 1 \ldots F$, and taking its real and imaginary parts, a linear system of $2NF$ equations in the $2NF$ unknowns q_{kljh}, $k = 1 \ldots N$, $l = 1, 2$, $j = 1 \ldots F$, is obtained, to

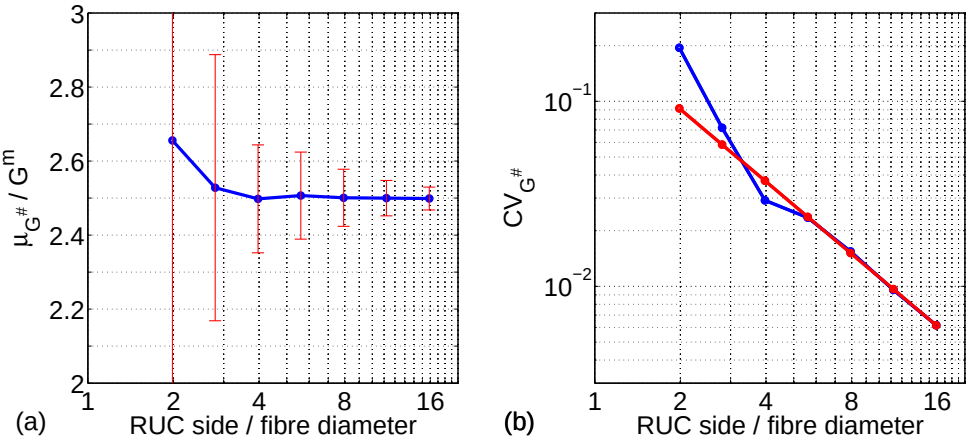

Figure 2: (a) Mean value $\mu_{G^\#}$ and dispersion of $G^\#$, normalized by $G^{\rm m}$, and (b) coefficient of variation $\mathrm{CV}_{G^\#}$, as a function of the RUC size. Monte Carlo simulation - blue line; fit reported in (46) - red line. Fibre/matrix stiffness ratio $G^{\rm r}/G^{\rm m} = 1000$. Grading type: exponential profile $g(\rho) = \exp(-\log(10)\rho^4)$. Isotropic fibres. Perfect interfaces. Square RUC. Volume fraction $f = 0.4$.

be solved for $h = 1$ and $h = 2$. Moreover, the truncation order N may be chosen for each fibre depending on its distance from neighbouring fibres. After computing q_{kljh}, one can determine w_{kljh} via (41), $b_{(-k)jh}$ via (37), and b_{kjh}, a_{kh} via (23). Hence, the cell functions $\chi^{\rm m}_h$, $\chi^{\rm f}_h$ are obtained by (16)–(17), for $h = 1, 2$.

Finally, the effective material tensor $\boldsymbol{G}^\#$ follows from (14). After some algebra, it turns out that:

$$G^\#_{hl} = G^{\rm m}\delta_{hl} + \sum_{j=1}^{F} \frac{f_j}{R_j} \Re\left[G^{\rm m}(\overline{c}_h b_{1jl} + c_h b_{-1jl}) - G^{\rm r}_j \Psi_j \overline{c}_h a_{1jl}\right] , \tag{43}$$

where $f_j = \pi R_j^2/|Q|$ is the volume fraction of the $j^{\rm th}$ fibre, and

$$\Psi_j = g_j(1) - \int_0^1 [\rho_j g_j'(\rho_j) + (1-\sigma_j^2) g_j(\rho_j)] W_{1j}(\rho_j)\, \mathrm{d}\rho_j \, . \tag{44}$$

For a general grading profile, the above coefficients Ψ_j, as well as the coefficients $W_{1j}(1)$ entering (24)–(25), can be computed via numerical integration of (18)–(20). Closed-form solutions to the latter problem for large families of grading profiles are presented in [15].

4 NUMERICAL RESULTS AND DISCUSSION

4.1 *The size of the RUC*

Statistically homogeneous microstructures, yielding an isotropic effective behaviour are considered. A quantitative estimation of the RUC size, based on statistical arguments, is derived here. The effective modulus $G^\#$, obtained by the spatial averaging (14) in a given RUC Q, is a random variable, since it depends on the specific realization of Q. If the RUC were a representative volume element (RVE), the dispersion would theoretically vanish. In practice, the RUC size has to be

chosen in order to ensure a given relative accuracy ϵ of $G^{\#}$. Recalling that the width of the 95% confidence interval is twice the standard deviation $\sigma_{G^{\#}}$ of $G^{\#}$, the following inequality must hold: $2\sigma_{G^{\#}}/\mu_{G^{\#}} \leq \epsilon$, where $\mu_{G^{\#}}$ denotes the mean value. In this way, large RUCs are usually obtained, whose analysis could require heavy computational effort.

However, the use of smaller RUCs might be compensated by averaging over several realizations of the microstructure to get the same accuracy, provided that no bias is introduced in the estimation by some edge effects generated by the periodic boundary conditions [2]. Indeed, the standard deviation of the average of $G^{\#}$ resulting from n independent realizations Q is given by $\sigma^n_{G^{\#}} = \sigma_{G^{\#}}/\sqrt{n}$, so that n could be chosen such that

$$n \geq 4\,\mathrm{CV}^2_{G^{\#}}/\epsilon^2\,, \tag{45}$$

where $\mathrm{CV}_{G^{\#}} = \sigma_{G^{\#}}/\mu_{G^{\#}}$ is the coefficient of variation.

It is pointed out that $\mu_{G^{\#}}$, $\sigma_{G^{\#}}$ and $\mathrm{CV}_{G^{\#}}$ do depend on the size of the RUC. An estimation of this dependence is obtained here in simulation. Square RUCs are considered, comprising equal, isotropic, graded fibres with volume fraction $f = \sum_{j=1}^{F} f_j = 0.4$, perfect fibre/matrix interfaces and stiffness ratio $G^{\mathrm{r}}/G^{\mathrm{m}} = 1000$. The RUC side S ranges from 1.98 to 15.85 fibre diameters (hence, the number of fibres included into a RUC ranges from 2 to 128).

Figure 2(a) shows the mean value $\mu_{G^{\#}}$ and the dispersion of $G^{\#}$ as a function of the RUC size. A bias in the mean value is observed when $S < 8$; on the other hand, a RUC whose side is greater than or equal to 8 fibre diameters (hence, comprising at least 32 fibres, for $f = 0.4$) can be used to obtain a fair estimate of $\mu_{G^{\#}}$ in the present case. Figure 2(b) shows the coefficient of variation $\mathrm{CV}_{G^{\#}}$ as a function of the RUC size. The empirical fit

$$\mathrm{CV}_{G^{\#}} \approx 0.27 \cdot S^{-1.5} \tag{46}$$

is obtained in the present case. Equations (45) and (46) can be used to estimate the number of realizations needed to reach a required accuracy. As an example, if $S = 8$, the estimated values derived from $n \geq 6$ RUC samples should be averaged in order to reach an accuracy of $\epsilon = 1\%$ on $\mu_{G^{\#}}$.

Further research will be devoted to ascertain how the present result depend on the fibre volume fraction, on the local randomness of the latter, on the fibre/matrix stiffness ratio or interface parameter, on the grading profile, and on the investigated effective property.

4.2 *The shear stress concentration factor*

In this section, the analysis points at assessing the reduction of the shear stress at the fibre/matrix interface, by suitably choosing the grading intensity factor $\omega = g(1)/g(0)$, keeping fixed the effective shear stiffness of the composite material.

Reference is made to a material with fibre volume fraction $f = 0.7$. Perfect interfaces are assumed. An exponential grading profile $g(\rho) = \exp(-\log(\omega)\rho^4)$ is considered, with $\omega = 1 \ldots 10$. Taking $\omega = 1$ amounts to considering standard homogeneous fibres. Square RUCs with edge length of 8 fibre diameters are used and the average over $n = 32$ samples is taken in each computation.

The dimensionless effective shear stiffness $\mu_{G^{\#}}/G^{\mathrm{m}}$ is taken constant. Hence, the higher ω is, the higher $G^{\mathrm{r}}/G^{\mathrm{m}}$ has to be chosen, since higher values of ω imply a steeper decrease of the fibre stiffness along the radius. This issue is shown in Figure 3(a), reporting the values of $G^{\mathrm{r}}/G^{\mathrm{m}}$ versus ω, that yield $\mu_{G^{\#}}/G^{\mathrm{m}} = 3$, 4 or 5.

Grading the fibre stiffness turns out to be a feasible way to mitigate the fibre/matrix interface shear stress. A quantitative account of this issue can be obtained by introducing the Shear Stress Concentration Factor (SSCF), defined as the highest ratio between the L^∞ norm of the normal

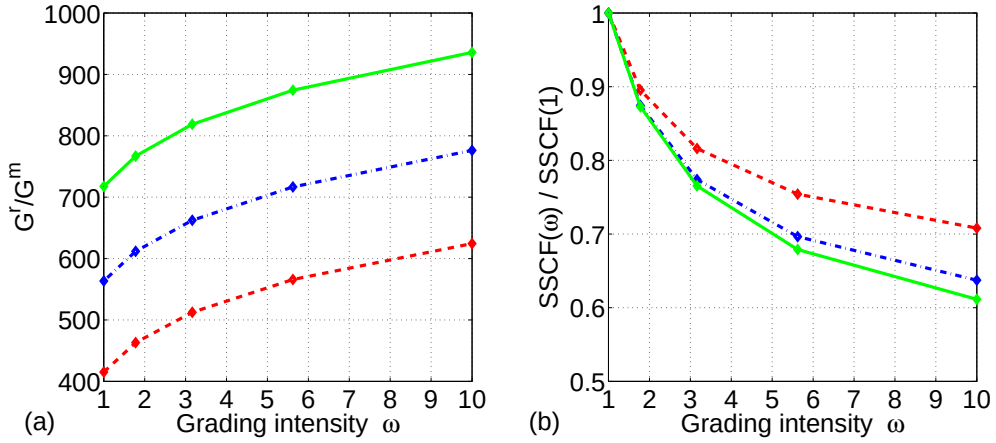

Figure 3: (a) Fibre/matrix stiffness ratio ($G^{\mathrm{r}}/G^{\mathrm{m}}$) required to achieve a given dimensionless effective modulus $\mu_{G\#}/G^{\mathrm{m}}$, vs grading intensity ω. (b) Normalized Shear Stress Concentration Factor [SSCF(ω)/SSCF(1)], vs grading intensity ω. $\mu_{G\#}/G^{\mathrm{m}} = 3$ - red dashed lines, $\mu_{G\#}/G^{\mathrm{m}} = 4$ - blue dash-dot lines, $\mu_{G\#}/G^{\mathrm{m}} = 5$ - green solid lines. Grading type: exponential profile $g(\rho) = \exp(-\log(\omega)\rho^4)$. Isotropic fibres. Perfect interfaces. Square RUC. Volume fraction $f = 0.7$.

component of the shear stress at the fibre/matrix interface in the graded composite, and the same quantity in the homogenized material, under all the macroscopic shear strains $\nabla_x w_0$:

$$\mathrm{SSCF} = \sup_{\nabla_x w_0} \frac{\sup\limits_{j\in\{1\ldots F\}} \sup\limits_{\rho_j=1} |\boldsymbol{\tau}_0 \cdot \boldsymbol{\nu}|}{G^{\#}|\nabla_x w_0|}\,. \tag{47}$$

This quantity is indeed a random variable: since it describes a stress level, its mean value increased by twice its standard deviation is considered. The SSCF(ω) for a composite comprising graded fibres, normalized by the corresponding SSCF(1) relevant to a composite with homogeneous fibres, is reported in Figure 3(b) as a function of ω, for $\mu_{G\#}/G^{\mathrm{m}} = 3$, 4 or 5. A reduction of the shear stress of 30% – 40% for highly graded fibres ($\omega = 10$) is observed for all the levels of dimensionless homogenized modulus. Hence, properly grading the elastic properties of the fibres leads to a decrease of the interfacial stress concentration, without reducing the overall stiffness of the material. This result raises attention on an innovative class of composite materials, enhanced in terms of durability of the bonding at the fibre/matrix interface.

References

[1] S. Suresh, "Graded materials for resistance to contact deformation and damage," *Science*, vol. 292, pp. 2447–2451, 2001.

[2] T. Kanit, S. Forest, I. Galliet, V. Mounoury, and D. Jeulin, "Determination of the size of the representative volume element for random composites: statistical and numerical approach," *Int. J. Solids Struct.*, vol. 40, pp. 3647–3679, 2003.

[3] Lord Rayleigh, "On the influence of obstacles arranged in rectangular order upon the properties of a medium," *Phil. Mag.*, vol. 34, pp. 481–502, 1892.

[4] T. Chen and H.-Y. Kuo, "Transport properties of composites consisting of periodic arrays of exponentially graded cylinders with cylindrically orthotropic materials," *J. Appl. Phys.*, vol. 98, p. 033716, 2005.

[5] P. Bisegna and F. Caselli, "A simple formula for the effective complex conductivity of periodic fibrous composites with interfacial impedance and applications to biological tissues," *J. Phys. D: Appl. Phys.*, vol. 41, p. 115506 (13pp), 2008.

[6] F. Lene and D. Leguillon, "Homogenized constitutive law for a partially cohesive composite material," *Int. J. Solids Struct.*, vol. 18, pp. 443–458, 1982.

[7] Z. Hashin, "The spherical inclusion with imperfect interface," *J. Appl. Mech.*, vol. 58, pp. 444–449, 1991.

[8] D. Bigoni, S. K. Serkov, M. Valentini, and A. B. Movchan, "Asymptotic models of dilute composites with imperfectly bonded inclusions," *Int. J. Solids Struct.*, vol. 35, no. 24, pp. 3239–3258, 1998.

[9] M. Amar, D. Andreucci, P. Bisegna, and R. Gianni, "On a hierarchy of models for electrical conduction in biological tissues," *Math. Meth. Appl. Sci.*, vol. 29, pp. 767–787, 2006.

[10] A. Bensoussan, J.-L. Lions, and G. Papanicolau, *Asymptotic Analysis for Periodic Structures*. Amsterdam: North-Holland, 1978.

[11] E. Sanchez-Palencia, *Non-Homogeneous Media and Vibration Theory*. Lecture notes in physics, Berlin: Springer, 1980.

[12] W. T. Perrins, D. R. McKenzie, and R. C. McPhedran, "Transport properties of regular arrays of cylinders," *Proc. R. Soc. Lond. A*, vol. 369, pp. 207–225, 1979.

[13] S. A. Meguid and A. L. Kalamkarov, "Asymptotic homogenization of elastic composite with a regular structure," *Int. J. Solids Struct.*, vol. 31, no. 3, pp. 303–316, 1994.

[14] R. Rodríguez-Ramos, F. J. Sabina, R. Guinovart-Díaz, and J. Bravo-Castillero, "Closed-form expressions for the effective coefficients of a fiber-reinforced composite with transversely isotropic constituents - I. Elastic and square symmetry," *Mech. Mater.*, vol. 33, pp. 223–235, 2001.

[15] E. Artioli, P. Bisegna, and F. Maceri, "Effective longitudinal shear moduli of periodic fibre-reinforced composites with radially-graded fibres," 2009. submitted.

[16] E. T. Whittaker and G. N. Watson, *A Course of Modern Analysis*. Cambridge: Cambridge University Press, 1927.

[17] T. M. Apostol, *Modular Functions and Dirichlet Series in Number Theory*. New York: Springer-Verlag, second ed., 1997.

[18] N. A. Nicorovici, R. C. McPhedran, and G. W. Milton, "Transport properties of a three-phase composite material: the square array of coated cylinders," *Proc. R. Soc. Lond. A*, vol. 442, pp. 599–620, 1993.